ORIGINAL ARTICLE

The effect of activator type on physicochemical and sorption properties of nanostructured carbon adsorbents obtained from fennel seed by chemical activation

Dorota Paluch[1] · Aleksandra Bazan-Wozniak[1] · Robert Pietrzak[1]

Abstract

In this study, fennel (*Foeniculum vulgare*) seeds were used as a precursor for obtaining nanostructured activated carbons by chemical activation with various reagents. The obtained activated carbons were characterized using nitrogen adsorption–desorption isotherms, ash content, Boehm titration and pH of water extracts. It was shown that the choice of activator had an important effect on the physicochemical and sorption properties of the obtained activated carbons. The specific surface area of the obtained adsorbents ranged from 345 to 1052 m^2/g. Chemical activation of the starting material with potassium carbonate made it possible to obtain activated carbons with the strongest developed specific surface area and the best sorption capacity against the tested pollutants. 1 g of this carbon is able to adsorb 1215 mg of iodine and 454 mg of methylene blue. The least effective adsorbent turned out to be the carbon obtained by chemical activation of fennel seeds with sodium carbonate, whose sorption capacity toward the pollutants from aqueous solutions was 77 mg/g and 317 mg/g for methylene blue for iodine, respectively. The alkaline pH of the solution promotes effective adsorption of methylene blue on the surface of the obtained adsorbents. The reaction of the dye molecules adsorption on the activated carbons occurs according to the pseudo-second-order model. The Langmuir isotherm best described the process under study. In addition, it was shown that chemical activation of fennel seeds leads to carbon adsorbents with acidic surface character. The negative values of Gibbs free energy indicate the spontaneous character of the process. The study has shown that fennel seeds can be successfully used to obtain low-cost and effective nanostructured carbon adsorbents with good sorption capacity toward organic and inorganic contaminants, from the aqueous phase.

Keywords Nanostructured activated carbon · Fennel seeds · Chemical activation · Methylene blue · Kinetics · Thermodynamic study

Introduction

Rapid development of textile industry is directly related to increasing pollution of fresh water bodies. It is anticipated that the waste generated by industry will increase at a geometric rate. Synthetic dyes have been used in textile industry for nearly 200 years (Ikram et al. 2022). They are chemical compounds of complex structure, showing high resistance to temperature, light and oxidizing substances. The presence of organic dyes in water reservoirs disturbs the penetration of light and thus the process of photosynthesis, which eventually results in reducing the content of oxygen (Vilén et al. 2022).

Thanks to its excellent physicochemical properties suitable for the purpose of adsorption, the most popular and highly effective sorbent is activated carbon. Its production as well as the demand for it, have been increasing from one year to another (Vilén et al. 2022). Activated carbon may be obtained by physical or chemical activation. The former process is realized in two steps. The first step is carbonization which is a thermal decomposition of a precursor containing carbon in organic connections, taking place in a neutral gas environment. The obtained carbonizate is subjected to activation with an activating gas, at a high temperature, in order to oxidize the carbonizate surface. The activating gas

✉ Aleksandra Bazan-Wozniak
  aleksandra.bazan@amu.edu.pl

[1] Faculty of Chemistry, Adam Mickiewicz University in Poznań, Uniwersytetu Poznańskiego 8, 61-614 Poznań, Poland

may be carbon(IV) oxide, oxygen or steam (Naji et al. 2022). Chemical activation is a single step process in which the precursor is impregnated with an activator (sodium or potassium carbonate, phosphoric(V) acid solution, zinc chloride or a sodium hydroxide) and then subjected to thermochemical treatment in a neutral gas atmosphere (Heidarinejad et al. 2020). The above-mentioned activators show high reactivity, which permits skipping the stage of carbonization, use of much lower temperature of the process and shortening of the time of activation. As each of the activators mentioned is characterized by a specific reactivity toward the precursor, the obtained activated carbons show different physicochemical properties (Kahn et al. 2019). According to the Lewis theory, the activators H_3PO_4 and $ZnCl_2$ are acids and react with the oxygen functional groups present on the surface of the activated material. The reactions catalyze the processes of dehydration and dehydrogenation that lead to pyrolysis of the precursor (Gao et al. 2020). Impregnation with phosphoric(V) acid at first leads to hydrolysis of glycoside bonds in hemicellulose of the precursor, followed by degradation, dehydration and condensation of the precursor accompanied by intensive liberation of carbon oxide and methane (Naji et al. 2022). When using potassium carbonate as an activator, it is known to reduce to K, K_2O, CO and CO_2, in a neutral environment. In the process of activation, potassium compounds penetrate the carbon structure and through chemical reactions enlarge the precursor pores (Foo et al. 2012). The use of sodium carbonate usually leads to material of poorer textural parameters, although this activator has a similar mechanism of activity (Heidarinejad et al. 2020). Chemical activation, although involving much higher cost and characterized by lower yield than the physical alternative, is often much more effective as it leads to getting adsorbents showing more developed porous structure and greater effectiveness in removing liquid or gas pollutants (Heidarinejad et al. 2020).

The precursors that may be used for production of activated carbons range from materials of animal origin (BalAltuntaş et al. 2020) to those of plant origin, including residues of supercritical extraction (Bazan-Wozniak et al. 2022), fruit stones(Cabrita et a. 2010) and easy to grow plants cultivated on a large scale (Kahn et al. 2019). The number of papers concerning the production of activated carbon has been continually increasing over the last decades (Bhattacharya et al. 2023; Bazan-Wozniak et al. 2022).

Production of fennel (*Foeniculum vulgare*) in Europe reaches over 600 000 tonsper year and is run mainly in Italy, France, Spain, Germany and the Netherlands(Shurr et al. 2022). Funnel seeds have found application in a wide range of areas, including gastronomy, perfumery and pharmaceutical industry as funnel seeds extract shows antiseptic and purgative properties as well as helps alleviate cough. According to recent studies, fennel extract may also be an alternative to antibiotics (Khan et al. 2022a, b). The properties of fennel seeds, their characteristic structure and their high availability make them attractive candidate for a precursor for activated carbon production. This realization inspired us to make an attempt at obtaining activated carbon by chemical activation of the residues of supercritical extraction of fennel seeds. The obtained products were characterized by determination of specific surface area, number of oxygen functional groups, pH of the activated carbons aqueous solutions, their elemental composition and content of mineral admixtures. Sorption capacities of the obtained activated carbons toward organic and inorganic pollutants of liquid phase: methylene blue and iodine, were determined. The methylene blue adsorption was also characterized by kinetic and thermodynamical studies.

Materials and methods

Materials

The precursor used for obtaining activated carbons were the residues of fennel seeds supercritical extraction. This material was characterized by the content of volatile matter of 7.89 wt%, moisture content of 5.27 wt% and ash content of 5.83 wt%. Prior to any treatment the precursor was dried for 24 h and then it was subjected to chemical activation with either of the three activators: sodium carbonate, potassium carbonate or a 50% solution of phosphoric (V) acid. Adsorption properties of the obtained activated carbons were tested toward methylene blue (MB) representing organic pollutants and iodine representing inorganic ones. Reagents were of analytical grade and were purchased from Merck (Darmstadt, Germany). Deionized water was used for the preparation of the solutions.

Preparation of activated carbons

The dry precursor was divided into three portions and each of them was impregnated with one of the three activators Na_2CO_3 (sample labeled as AC_{Na}), K_2CO_3 (labeled as AC_K) or a 50% solution of H_3PO_4 (labeled as AC_P). For all activators, the impregnation ratio of precursor to activator was 1:2. Samples of impregnated precursors were placed in a tube furnace and heated from room temperature to 500 °C—sample AC_P or to 700 °C—samples AC_{Na} and AC_K. After reaching the target temperature, the samples were thermostated for 45 min. The chemical activation was carried out in a nitrogen atmosphere blown at a rate of 330 mL/min. After the process, the samples were cooled to room temperature in a neutral atmosphere. Samples AC_{Na} and AC_K were washed at first with a hot 5% solution of hydrochloric acid and then to neutralize the material, with about 10 L

of boiling distilled water until getting a neutralized filtrate. Sample AC_P was washed only with boiling distilled water. The activated products were dried to constant mass.

Biocarbons characterization

Textural properties of the obtained samples were characterized on the basis of isotherms of nitrogen adsorption/desorption measured at 77 K using an AutosorbiQ analyzer from Quantachrome Instruments (Boynton Beach, FL, USA). Prior to measurements of nitrogen adsorption, the carbon samples were degassed in vacuum for 12 h at 300 °C. The surface area of the samples was calculated from the appropriate isotherm of nitrogen adsorption, according to the Brunauer, Emmett, Teller method. The total pore volume (V_T) was determined on the basis of the volume of adsorbed nitrogen at the relative pressure $p/p_0 = 0.99$, which is obtained by dividing the equilibrium pressure by saturation pressure and expressed for the volume of adsorbed nitrogen in liquid state at a given temperature. The mean pore diameter (D) was calculated from the equation: $D = 4V_T/S_{BET}$, where S_{BET} is the specific surface area of the carbon samples. The pores were assumed to be of cylindrical shape. The ash content was determined by a standard method, according to the norm ASTM D2866-94 (2004). Thermo Scientific FLASH 2000 Elemental Analyzer was employed to establish the elemental composition of precursor and biocarbons.

The content of surface oxygen functional groups of basic or acidic character was determined for both the precursor and the activated carbon samples (Mahardiani et al. 2019). Values of pHof water extracts of all samples were measured using a pH-meter made by Elmetron, model CP—401.For the obtained activated carbon samples also the iodine number was determined (Bazan 2017).

Adsorption of methylene blue

Methylene blue (MB), analytical grade, was purchased from Merck (Darmstadt, Germany). Stock solution of MB was made in concentration of 1000 mg/L and it was used to make solutions of concentrations in the range 10–200 mg/L. To evaluate the adsorption capacities of the activated carbon samples toward MB, 25 mg of each sample was mixed with 50 mL of an MB solution of a proper concentration. The samples with MB solution were shaken for 24 h on a shaker (Heidolph, Schwabach, Germany) at the rate of 200 rpm/min. Then, the samples were taken out with a syringe and centrifuged for 10 min in a laboratory centrifuge (OHAUS, Parsippany, USA). The concentration of methylene blue in the solution was measured spectrophotometrically at λ_{max} 665 nm, using a Carry 100 Bio spectrophotometer, (Agilent, SantaClara, CA, USA). The amount of MB (q_e) adsorbed on the samples studied was calculated from the equation:

$$q_e = \frac{C_0 - C_e}{m} \times V$$

where: C_0–the initial concentration of MB solution, [mg/L]; C_e –the concentration of MB in the solution at equilibrium [mg/L]; m-the mass of the activated carbon sample [g]; V –the volume of MB solution MB [L].

The effect of pH (varied in the range 3–11) of the aqueous solution of MB on the sorption capacities of the activated carbon samples was tested (BlueLine 25 pH electrode (SI Analytics, Weilheim, Germany). Measurements were performed for the biocarbon samples of 25 mg. Each of the samples was flooded with 50 mL of the aqueous solution of MB. The MB concentrations were of 50 mg/L for samples AC_{Na} and AC_P, and 150 mg/L for sample AC_K. The effect of temperature of adsorption on the adsorption capacities of the activated carbon samples toward MB was also studied. Biocarbon adsorbent samples AC_{Na} and AC_P of 25 mg were flooded with 40 mg/L MB, while sample AC_K was flooded with 200 mg/L MB. Sorption of MB on activated carbon samples was run at three temperatures of 25, 45 and 60 °C. To study the effect of pH of the dye solution and temperature on the sorption capacity of the activated carbon samples, the flooded samples were shaken for 24 h on a shaker (Heidolph, Schwabach, Germany) at the rate of 200 rmp/min. After this time, spectrophotometric measurements were made.

Two models, proposed by Langmuir and Freundlich, were considered in order to establish the mechanism of MB adsorption on the samples studied (Table 1).

According to the Langmuir model, on the adsorbent surface there is a specific number of active sites, the so-called adsorption sites, each of which is able to adsorb one molecule of adsorbate, so that an adsorption monolayer of adsorbate molecules is formed. The model assumes no interactions between the adsorbate molecules (Canales-Flores et al. 2020). According to the Freundlich model, a multilayer of the adsorbent molecules is formed on the adsorbent surface. The Freundlich model is used for description of heterogeneous systems (Ezzati et al. 2020).

In order to characterize the kinetics of adsorption of MB from an aqueous solution on the activated carbon samples, two kinetic models were considered: that of pseudo-first order proposed by Lagergren and pseudo-second order proposed by Ho&McKay (Table 2) (Tien et al. 2017).

In the Lagergren model, the adsorption rate is directly proportional to the difference between the equilibrium and temporary concentration the adsorbate adsorbed on the adsorbent (Tien et al. 2017). The model proposed by Ho&McKay describes the rate of occupation of the available active centers by the adsorbate, which is proportional to the square of the number of free adsorption sites (Tien et al. 2017). The experimental adsorption studies were conducted

Table 1 Equations describing the models of adsorption proposed by Langmuir and Freundlich

Isotherms model	Linear equation	Parameters
Langmuir	$\frac{C_e}{q_e} = \frac{1}{K_L \times q_{max}} + \frac{C_e}{q_{max}}$	C_e—dye concentration in solution after the adsorption [mg/L], q_e—amount of adsorbed dye [mg/g], K_L—Langmuir constant [L/mg], q_{max}—sorption capacity of the monolayer [mg/g]
Freundlich	$log q_e = log K_F + \frac{1}{n} \times log C_e$	q_e—amount of adsorbed dye [mg/g], K_F—Freundlich constant [mg/g(L/mg)$^{1/n}$], 1/n—a constant related to the adsorbate affinity to adsorbent, C_e—dye concentration in solution after adsorption [mg/L]

in triplicate, and the results are presented with the standard deviation.

Results and discussion

Elemental analysis

Table 3 presents results of elemental analysis of the precursor and activated carbons obtained in the study. Dry fennel seeds contain nearly 51 wt% of elemental carbon. The content of sulfur and hydrogen is much lower in the activated carbon samples than in the precursor. After pyrolysis of the precursor, the content of elemental carbon increased by 21–27% points. Chemical activation of the precursor led to a decrease in the contents of oxygen, sulfur and hydrogen in the activated carbon samples. Upon activation of the precursor, sulfur oxides and hydrides were released, leading to a decrease in the contents of these elements in the activated

elemental analysis, the highest percentage of carbon was obtained for the sample activated with potassium carbonate (AC$_K$), while the lowest—for the sample activated with phosphoric(V) acid (AC$_P$). Another conclusion from Table 3 data is that the use of carbonates as activators led to the adsorbents of greater content of nitrogen.

The ash content in fennel seeds reaches 5.8 wt.%, while the content of mineral substance in the activated carbon samples varied from 0.2 to 11.7 wt% (Fig. 1). The activated carbon obtained as a result of the precursor activation with potassium carbonate contained only 0.2 wt% of ash. For comparison, the activated carbon obtained by chemical activation of peach stones with potassium carbonate (Cabrita et al. 2010)contained 13 wt% of ash, which is 65 times more than sample AC$_K$. The content of ash in sample AC$_{Na}$, activated with sodium carbonate was 2.7 wt%. Sample AC$_P$, obtained by activation of fennel seeds with a 50% solution of H$_3$PO$_4$, contained far more mineral substance than the other samples. The activated carbon obtained

Table 2 Models of adsorption kinetics

Kinetics model	Linear equation	Parameters
Pseudo-1st order	$log\left(q_e - q_t\right) = log q_e - \frac{k_1}{2,303}t$	q_e–amount of adsorbed dye at equilibrium [mg/g], q_t—amount of dye adsorbed in a given time [mg/g], t—time [min], k_1—constant of pseudo-first order adsorption [1/min]
Pseudo-2nd order	$\frac{t}{q_t} = \frac{1}{k_2 q_{e2}} + \frac{t}{q_e}$	q_e—amount of adsorbed dye at equilibrium [mg/g], q_t—amount of dye adsorbed in a given time [mg/g], t –time [min], k_2—adsorption rate constant of pseudo-second order reaction [g/mg×min]

carbon samples (Sekirifa et al. 2013). As follows from the

from barley husk chemically activated with orthophosphoric

Table 3 Elemental analysis of the precursor and activated carbon samples and yield of the activation processes

Sample	% N	% C	% H	% S	% O	Yield%
Fennel	3.32	50.85	7.71	0.66	37.46	–
AC$_{Na}$	3.70	75.38	2.58	0.16	18.18	32.28
AC$_K$	2.80	77.96	1.96	0.11	17.17	29.12
AC$_P$	1.31	72.54	2.79	0.18	23.18	42.21

Fig. 1 The content of ash in the precursor and activated carbon samples obtained from it
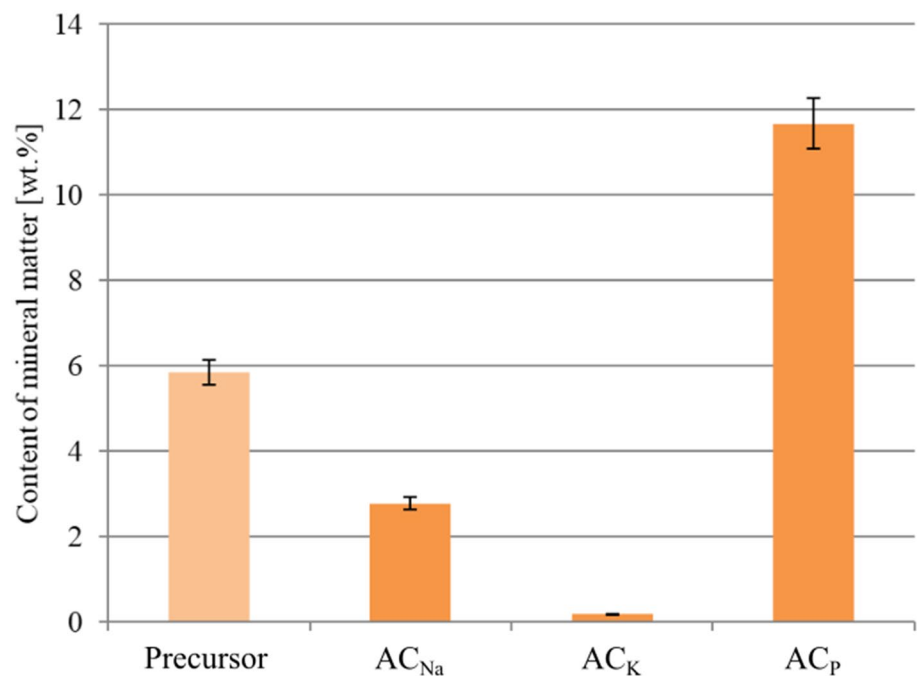
acid (Canales-Flores et al. 2020) showed the ash content of 11.9 wt%, while the adsorbents obtained from corn cob and *Agave salmiana* leaves contained only 3.1 and 1.1 wt% of ash, respectively. In view of the above literature data, it may be concluded that the choice of precursor determines the content of mineral substance in the final product. The activated carbon samples obtained by chemical activation of fennel seeds with sodium and potassium carbonates were washed with a 5% solution of HCl in order to wash out the unreacted carbonates (Sevilla et al. 2021), while the sample activated with phosphoric (V) acid washed only with hot water, which shows that the type of washing may also affect the content of ash in the adsorbents. According to Fig. 1, the two-stage washing of samples AC_K and AC_{Na} leads to adsorbents of low content of ash composed mainly of inorganic compounds like mixtures of alkali metal oxides and their carbonates or salts (Vassilev et al. 2013).

Physiochemical properties of the obtained activated carbons

According to Table 4, the total surface area of the activated carbon samples varies from 345 to 1052 m^2/g. Textural parameters of the obtained adsorbents depend on the type of activator used. The specific surface area of samples AC_P and AC_{Na} is 518 and 345 m^2/g, respectively. Particularly interesting is sample AC_K showing the best textural parameters: specific surface area of 1052 m^2/g, large pore volume of 0.678 cm^2/g and high ratio of the volume of micropores to the total pore volume (80%). For comparison, the commercial adsorbent Norit SX2 has the specific surface area of 1092 m^2/g (Bazan-Wozniak et al. 2022).The well-developed porous structure of sample AC_K is related to the mechanism of activation with potassium carbonate. Sample AC_P shows the largest average pore diameter and the lowest ratio of micropores volume to the total pore volume.

Figure 2 presents the isotherms of low-temperature nitrogen adsorption/ desorption and pore size distribution

Table 4 Textural parameters of activated carbons

Sample	Surface area [m^2/g]		Pore volume [cm^3/g]		V_m/Vt	Average pore size[nm]
	Total	Microporous	Total	Microporous		
AC_{Na}	345	302	0.349	0.165	0.473	4.04
AC_K	1052	1002	0.678	0.544	0.802	2.58
AC_P	518	331	0.637	0.180	0.283	4.92

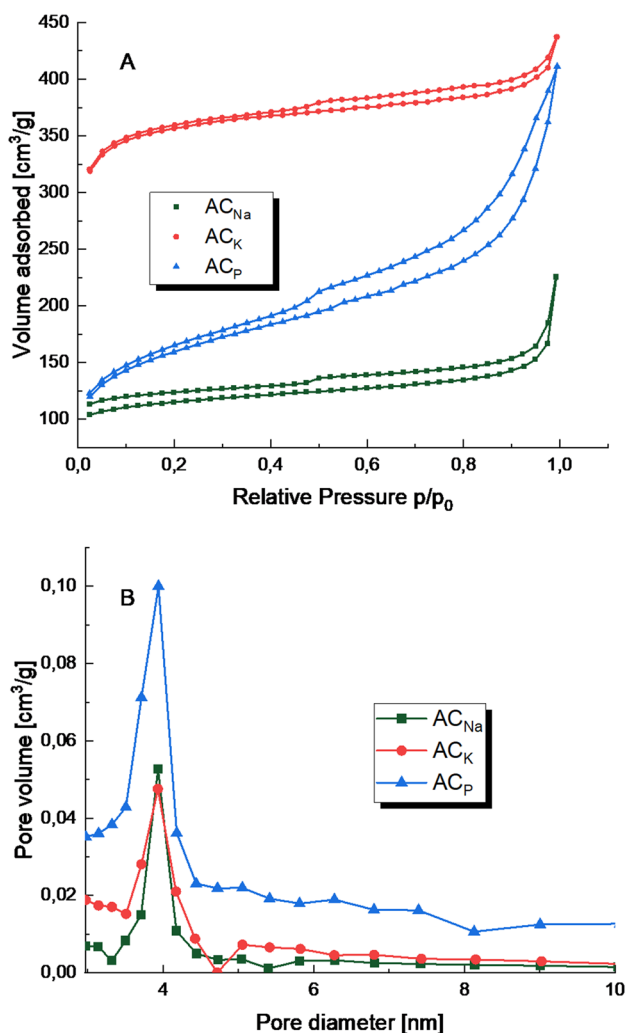V_m—micropore volume, V_t—total pore volume

Fig. 2 Low-temperature N_2 adsorption–desorption isotherms **A** and pore size distribution **B** of AC_{Na}, AC_K and AC_P samples

obtained for the activated carbon samples studied. The isotherms may be classified as type IV(a) (Thommes et al. 2015). The capillary condensation is accompanied by hysteresis which is known to occur for pores wider than ~4 nm. The IUPAC classification distinguishes six types of hysteresis loops closely related to the porous structure of the adsorbent and the mechanism of adsorption. For all activated carbon samples studied the hysteresis loops represent type H4, characteristic of materials containing narrow slit pores (Thommes et al. 2015), which is in agreement with the data presented in Table 4.

Further analysis of textural parameters shows that sample AC_P is characterized by the lowest ratio of the micropores volume to the total pore volume and the presence of pores of the greater average diameter. Moreover, chemical activation of fennel seeds leads to carbon adsorbents of microporous (AC_K) or micro-mesoporous (AC_{Na}, AC_P) surface character.

Table 5 presents the textural parameters and conditions of obtaining activated carbons from different precursors of plant origin as a result of chemical activation with orthophosphoric acid, sodium carbonate or potassium carbonate. A comparison of sample AC_P with the adsorbent obtained by chemical activation of lemon and orange peels with an 85% orthophosphoric acid (Ramutshatsha-Makhwedzha et al. 2022) shows that the latter has almost three times smaller total surface area than the former (obtained by fennel seeds activation with a 50% solution of this acid. Moreover, sample AC_P was obtained at a lower temperature and a much shorter time of thermostating. Thanks to these conditions, the process of obtaining of AC_P was cheaper, more ecological and more effective. Orthophosphoric acid acts as a catalyst, its presence facilitates bond cleavage reactions and favors crosslinking of the structure through cyclization, condensation and generation of phosphate and

Table 5 Comparison of textural properties of activated carbon samples obtained from different agricultural waste products subjected to chemical activation with different reagents

Precursor	Reagent	Activation temperature (°C)	Activation time (min)	Chemical ratio (activating agent/precursor) (g:g)	BET surface area (m²/g)	Pore volume (cm³/g)	References
Palm oil shell	Na_2CO_3	700	120	1	671	0.374	Hussaro et al. (2014)
		700	120	2	726	0.404	
		700	120	3	742	0.418	
Orange and lemon peels	85% H_3PO_4	600	180	1	168	-	Ramutshatsha-Makhwedzha et al. (2022)
Cassia fistula rose pods	K_2CO_3	800	240	1	1413	0.660	Canales-Flores et al. (2020)
Peach stones	K_2CO_3	700	60	1	866	0.385	Cabrita et al. (2010)
Fennel seed	K_2CO_3	700	45	2	1052	0.678	This study
	50% H_3PO_4	500	45	2	518	0.637	
	Na_2CO_3	700	45	2	345	0.349	

polyphosphate bonds. After its removal by washing out, polyphosphates leave unoccupied voids—pores. The higher the content of orthophosphoric acid in a system, the greater the amount of polyphosphates, and thus, the greater the volume of pores (Sych et al. 2012). However, when a too high concentration of orthophosphoric acid is used, the pore walls may become very thin and eventually collapse, leading to a decrease in pore volume and BET surface (Sych et al. 2012).

Hussaroet al. (2014) have studied a series of activated carbons obtained by chemical activation of oil palm shells with sodium carbonate at different weight ratios of activator to precursor. The activation temperature of all samples was 700 °C and the time of thermostating was 120 min. With increasing weight ratio of activator to precursor, the textural parameters of the obtained adsorbents were observed to improve. In comparison with the adsorbents obtained from oil palm shells, sample AC_{Na}, obtained from fennel seeds, has over twice smaller specific surface area and the pore volume smaller by 25–169 cm^3/g.

A comparison of sample AC_K with the adsorbents obtained from other precursors characterized in Table 5, shows that the activated carbon sample obtained from *Cassia fistula rose* (Tran et al. 2018) has specific surface area by almost 35% greater than sample AC_K obtained from fennel seeds using the same activator (potassium carbonate). However, the activated carbon sample from *Cassia fistula rose* was obtained at a temperature by 100 °C higher than that used to produce AC_K and in a thermostating time 5 times longer, which increased the time of the process, cost of sample production and was less ecological. The total pore volume of the above compared two samples was similar. The adsorbent obtained from peach stones (Cabritaet al. 2010) in similar activation conditions, showed the specific surface area by almost 200 m^2/g greater and the pore volume by about half smaller. Moreover, the adsorbent from peach

stones was heated for a longer time, which increased the cost of its production.

In order to characterize the acid–base properties of the precursor (fennel seeds) and the activated carbon samples obtained from it, the pH of their water extracts were measured and the number of surface oxygen functional groups was determined by the Boehm method, Fig. 3.

The water extract of fennel seeds has pH of 6.1 and contains more acidic than basic groups. Prevalence of acidic groups over basic ones was determined for each of the activated carbon sample obtained. The most acidic surface character, pH of 3.0, was found to have sample AC_P, obtained by fennel seeds activation with a 50% solution of H_3PO_4. The content of acidic surface oxygen functional groups on AC_P surface was 2.0 mmol/g, while that of basic groups was 0.6 mmol/g. The pH of water extracts of the activated carbon samples activated by potassium or sodium carbonates were higher. The content of acidic groups on sample AC_K surface was 1.75 mmol/g, while that of basic groups was 0.55 mmol/g. The analogous contents for sample AC_{Na} were 2.61 mmol/g (acidic groups) and 0.80 mmol/g (three times less basic groups). For comparison, Tran et al. (2018) have obtained activated carbon from *Cassia fistula rose* by chemical activation with potassium carbonate, that contained 2.12 mmol/g surface acidic groups and 1.56 mmol/g surface basic groups. Thus, it may be concluded that chemical activation of plant precursors (Tran et al. 2018; Bazan-Wozniak et al. 2018Doczekalska et al. 2022) predominantly gives activated carbons containing more acidic groups than basic ones on the surface. Acidic oxygen functional groups are formed upon oxidation of activated carbon at high temperatures and their presence is responsible for the polar and hydrophilic character of the carbon samples surface (Alves et al. 2016). Basic oxygen functional groups are formed as a result of oxygen chemisorption on the carbon samples
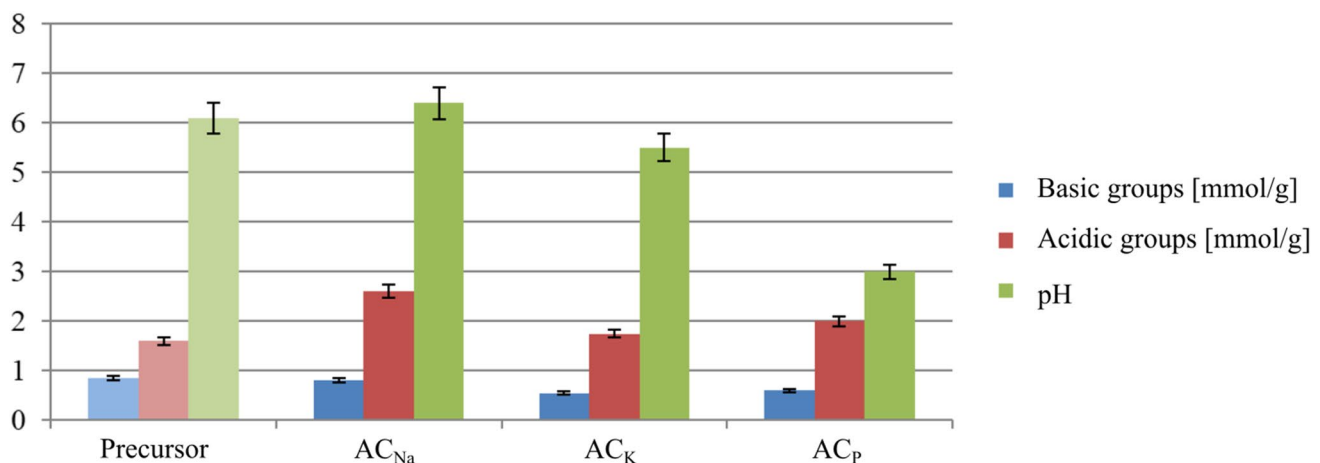

Fig. 3 The number of oxygen functional groups on the surface of the activated carbon samples studied and pH of the water extracts of the samples

surface at a high temperature and in the atmosphere of oxidizing gas (Alves et al. 2016). Therefore, basic character of the carbon samples surface is typical of samples obtained by physical activation of plant origin precursors (Heidarinejad et al. 2020).

Adsorption of iodine

The main aim of the study was evaluation of sorption abilities of the obtained activated carbon samples toward liquid pollutants, represented by methylene blue and iodine. The yield of adsorption depends on the physicochemical properties of both, adsorbate and adsorbent (Heidarinejad et al. 2020). The activated carbon properties determining the character of adsorption are: pore size, specific surface area and the presence of oxygen functional groups on the surface (Queiroz et al. 2020).

The iodine numbers of samples AC_P and AC_K were found to be 1196 and 1215 mg/g, respectively (Fig. 4). According to the results of their physicochemical studies, the specific surface area of samples AC_P and AC_K was more developed than that of sample AC_{Na} (Table 4), which is directly related to the lower value of the iodine number of the latter sample, of 317 mg/g. For comparison, the activated carbon sample obtained by chemical activation of hop cones with Na_2CO_3 (Bazan-Wozniak et al. 2018) is characterized by the specific surface area of 1048 m^2/g and the iodine number of 1278 mg/g. It should be noted that the iodine numbers of commercial activated carbon adsorbents F-300 and WG-12 are 850 mg/g and 1050 mg/g, respectively, so smaller than those obtained for samples AC_K and AC_P (Nowicki et al. 2015). The activated carbon obtained by activation of fennel seeds with a 50% solution of phosphoric (V) acid was found to show much higher sorption capacity toward iodine than it would be expected on the basis of its textural parameters (Table 4). Tounsadi et al. (2016) reported a similar result

for the activated carbon sample obtained from *Glebionis coronaria L.* biomass with orthophosphoric acid, using a precursor to activator mass ratio of 1:2. Specifically, one gram of this activated carbon had a specific surface area of 102 m^2/g and was able to adsorb 795 mg of iodine. Probably, the use of H_3PO_4 as an activator leads to the formation of such functional groups on the activated carbon surface that react with iodine molecules. Orthophosphoric acid may modify the carbon surface properties through introduction of phosphoric groups (Danish et al. 2022; Canales-Flores et al. 2020; Tounsadi et al. 2016). Perhaps this may be the reason why the iodine numbers of sample AC_P and the adsorbent obtained from *Glebionis coronaria L.* biomass were much higher than their textural parameters would imply.

Adsorption of methylene blue

On the basis of the results presented in Fig. 5 it follows that the most effective adsorbent toward methylene blue in aqueous solution proved to be sample AC_K obtained by precursor activation with potassium carbonate as an activator. The sorption capacity of this sample toward MB was 474 mg/g. For comparison, the activated carbon obtained by chemical activation of orange peel with potassium carbonate (Foo et al. 2012) of the specific surface area of 1104 m^2/g, was able to adsorb 380 mg/gof MB, so almost 100 mg/g less than sample AC_K.The latter sample has a well-developed specific surface area, microporous structure (Table 4) and very low ash content (Fig. 1), which are conducive to high sorption capacity. The sorption capacity of sample AC_{Na}, obtained by fennel seeds activation with sodium carbonate, is almost 6 times lower (77 mg/g) than that of sample AC_K. For comparison, the adsorbent obtained from oil palm leaves activated by a 10% solution of Na_2CO_3 (Cabrita et al. 2010) was able to adsorb 889 mg/g. As shown above, sample AC_{Na} was characterized by the least developed specific surface

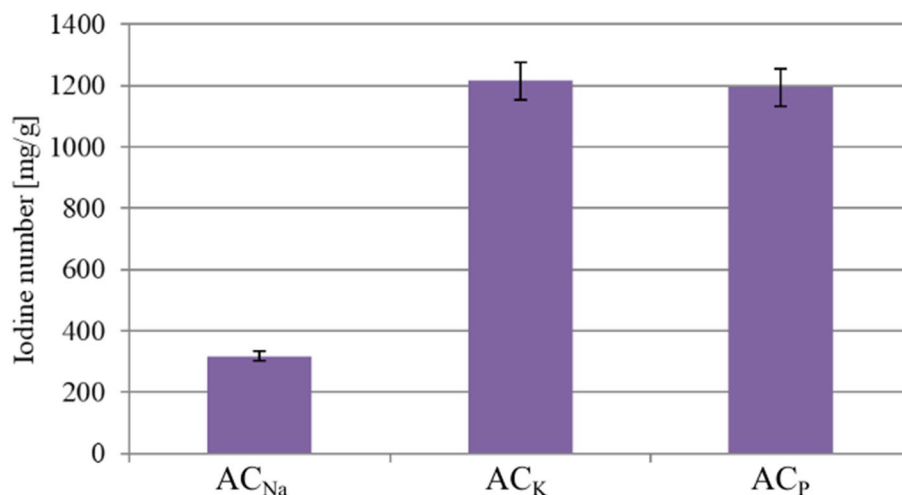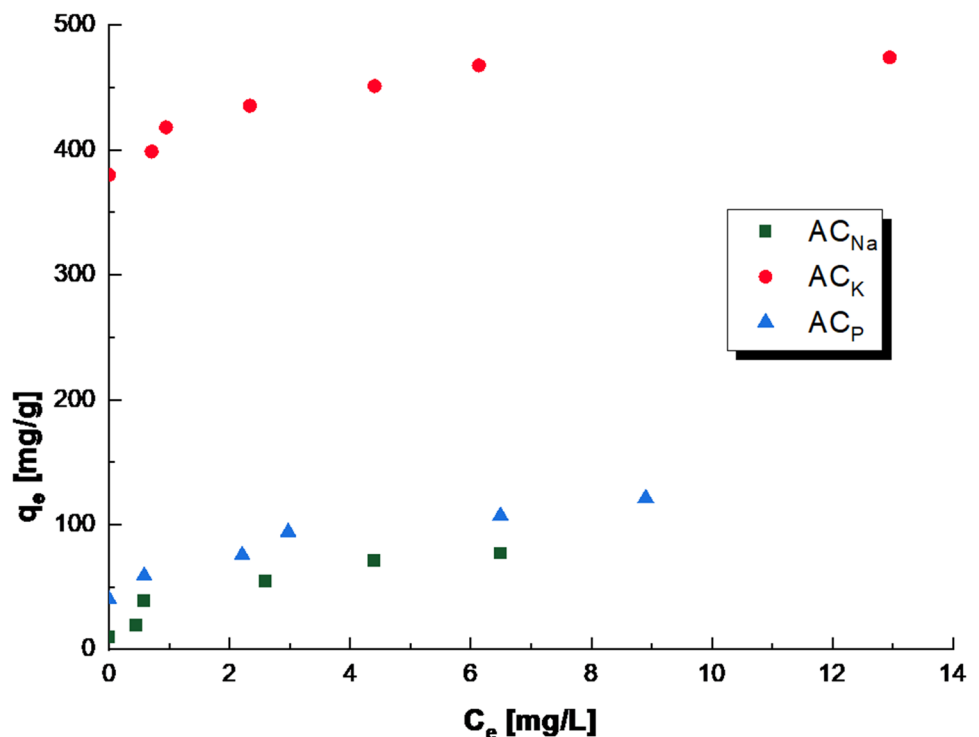**Fig. 4** Iodine numbers of the obtained activated carbons

Fig. 5 Isotherms of methylene blue adsorption on biocarbons (biocarbon mass: 25 mg, initial dye solution concentration: 5–45 mg/L for AC_{Na}, 20–70 mg/L for AC_P and 190–250 mg/L for AC_K, volume of methylene blue solution: 50 mL, temperature: 23 ± 1 °C)

area, which explains the much poorer sorption capacity of this sample. As follows from our study, 1 g of sample AC_Pis able to adsorb 122 mg/gof MB. This result can be compared with that of the adsorbent obtained from *Agave salmiana* leaves (Canales-Flores et al. 2020) by activation with phosphoric(V) acid, whose sorption capacity toward MB was 89 mg/g, which is close to 30% lower than that of sample AC_P.

Figure 6 presents results of the fit of the experimental data to the Langmuir and Freundlich models, assuming different mechanisms of interaction between the adsorbate and adsorbent. The model best fitting the experimental results provides information on the type of mechanism of interaction between adsorbents and MB. Tables 6 and 7 present the values of characteristic constants obtained from the experimentally determined linear and nonlinear isotherms. Figure 6 shows the linear fit of the Langmuir and Freundlich isotherms for the obtained ACs, while Fig. 7 shows the nonlinear fit. The values of q_{max} for the nonlinear Langmuir model are by 2–9 mg higher than the experimental q_e values. The correlation coefficient R^2 determined assuming the linear models is higher than that obtained for nonlinear ones. The character of the nonlinear curves of the Langmuir and Freundlich models does not allow a clear determination according to which model the adsorption process occurs.

The character of MB adsorption on the obtained activated carbon samples was best described by the linear versions of the Langmuir and Freundlich models. According to the data presented in Table 6, for all activated carbon samples the

correlation coefficient was higher for the fit with the Langmuir model. The highest correlation was obtained for sample AC_K (0.999), while the lowest for sample AC_P (0.973).

To sum up, it is reasonable to assume that the MB adsorption on activated carbons studied is described by the Langmuir model, which implies the formation of an adsorption monolayer on the adsorbent surface (Medhat et al. 2021; Ishak et al. 2022; Gupta et al. 2022).

In the Langmuir isotherm equation, the constant K_L defines the maximum amount of a substance that can be bonded to the adsorbent unit area at equilibrium, which is a measure of adsorption strength; the higher the K_L constant, the stronger the adsorption (Khan et al. 2022a, b). Thus, the sample AC_K shows the greatest affinity to the adsorbate (MB), while sample AC_{Na}—the lowest.

The constant 1/n in the Freundlich model informs about the system's inhomogeneity; the higher the constant, the greater the inhomogeneity (Al-Ghouti et al. 2020). The least heterogeneous is sample AC_{Na}, while the most heterogeneous is sample AC_K. The constant K_F obtained for Freundlich isotherms, is a measure of selectivity (Villabona-Ortíz et al. 2022) and it is the lowest for the sample of the poorest sorption capacity, AC_{Na}, while the highest for the sample of the greatest sorption capacity, AC_K.

pH effect

To maximize the yield of adsorption, the pH of the MB aqueous solution should be optimized. The value of pH has a
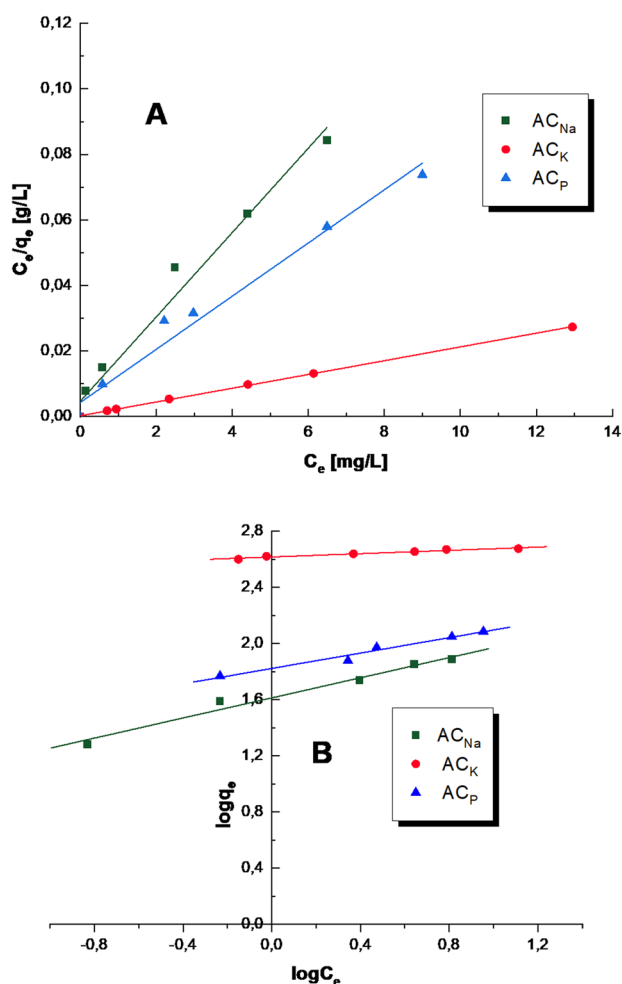
Fig. 6 Linear fitting of methylene blue adsorption isotherms on biocarbon adsorbents to Langmuir **a**, Freundlich **b** models

significant impact on the acidic and basic properties of activated carbon surface, so also on its ability to adsorb anionic and cationic dyes (Ishak et al. 2022). Figure 8 presents the

effect of pH of the aqueous solution of MB on its adsorption on the activated carbons obtained.

As presented in Fig. 8, the sorption capacities of the activated carbon samples studied slightly increase with increasing pH of the MB aqueous solution. Therefore, it may be concluded that the value of pH of the MB aqueous solution has minor effect on the sorption capacities of the activated carbon samples studied. It is economically beneficial as these samples are effective MB adsorbents in the whole range of pH studied. In other words, no optimization of pH of the MB solution is needed to get effective MB adsorption by the samples studied. A significant increase in the sorption capacity of activated carbons toward MB with increasing pH has been observed by Gupta et al. (2022) and Shiet al. (2022).This dependence is related to the fact that the pH of MB solution affects the charge on the adsorbate molecule and that on the adsorbent surface, which induces electrostatic interactions. The functional groups on the adsorbent surface may be protonated or deprotonated. The positive effect of increasing pH of MB solution on the activated carbons' sorption capacity is determined by the MB molecule properties. MB is a cationic dye and in aqueous solution its molecules have a positive charge. In the solution of basicpH, the hydroxyl ions tear away the protons of the oxygen functional groups on the activated carbon surface, leading to generation of negative charge on the adsorbent surface. It increases the affinity of MB molecules to the adsorbent surface and thus, its sorption capacity (Pathania et al. 2017).

Adsorption kinetics

The dependence of the amount of adsorbed dye on the time of contact of MB solution with the adsorbent is presented in Fig. 9. The experimental data were fitted with the pseudo-first order and pseudo-second order kinetic models, (Table 8). Adsorption of MB was very fast at the beginning

Table 6 The values of constants determined for the linear Langmuir and Freundlich models used for the fit of experimental data of MB adsorption

Sample	q_e [mg/g]	Langmuir			Freundlich		
		R^2	q_{max} [mg/g]	K_L [L/mg]	R^2	K_F [mg/g(L/mg)$^{1/n}$]	$1/n$
AC_{Na}	77	0.974	78	0.014	0.958	41.03	0.358
AC_K	474	0.999	476	0.035	0.978	413.71	0.059
AC_P	122	0.973	123	0.015	0.969	66.48	0.274

Table 7 The values of constants determined for nonlinear Langmuir and Freundlich models used for the fit of experimental data of MB adsorption

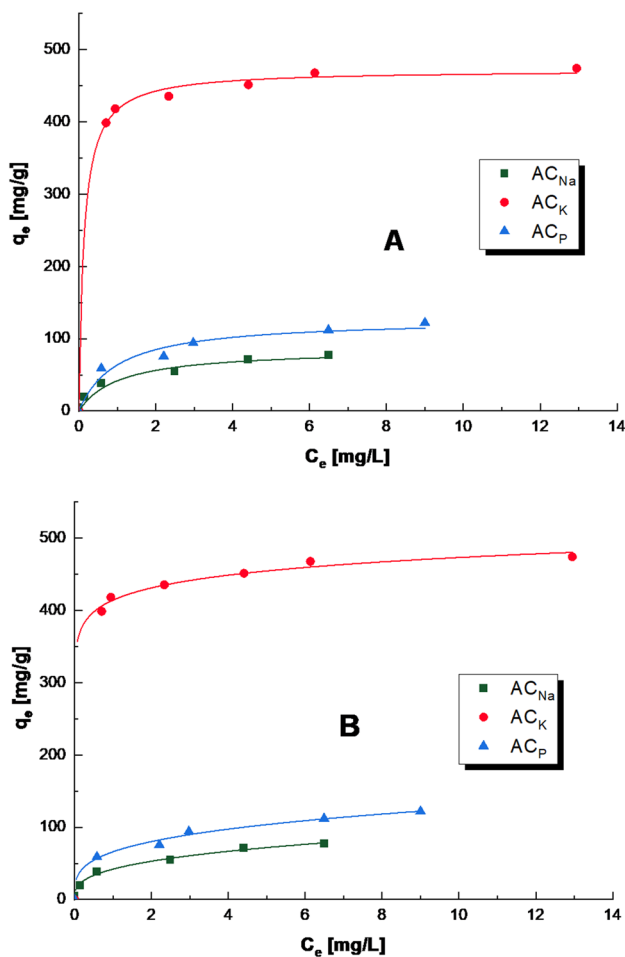| Sample	q_e [mg/g]	Langmuir			Freundlich		
		R^2	q_{max} [mg/g]	K_L [L/mg]	R^2	K_F [mg/g(L/mg)$^{1/n}$]	$1/n$
AC_{Na}	77	0.942	86	0.950	0.984	42.000	0.333
AC_K	474	0.998	472	7.570	0.958	414.103	0.058
AC_P	122	0.917	127	0.999	0.973	65.981	0.280

Fig. 7 Nonlinear fitting of methylene blue adsorption isotherms on biocarbon adsorbents to Langmuir **a**, Freundlich **b** models

of the process, then it gradually slowed down until reaching the state of equilibrium.

With increasing time of contact between the activated carbon samples and MB solution, no significant changes were noted in the samples sorption capacities. For the samples obtained by chemical activation of fennel seeds with potassium carbonate and those activated with a 50% solution of H_3PO_4, the state of equilibrium was reached in 10 to 20 s, for sample AC_{Na} it took about 180 min. It should be emphasized that for sample AC_K the maximum sorption capacity was experimentally determined in a very short time, which is economically beneficial. Peruse of literature reveals that in many adsorption processes it was necessary to run the process for a few h to reach the state of adsorption equilibrium (Pathania et al. 2017). A rapid increase in the MB adsorption at the beginning of the process is most probably a result of availability of many free adsorption sites on the adsorbents' surface (Misran et al. 2022).

The fit of Table 8 data to the pseudo-first order kinetic model is characterized by the correlation coefficient R^2

from the range 0.845–0.981, while the analogous fit to the pseudo-second order kinetic model is characterized by R^2 values not lower than 0.997. These values of the correlation coefficient imply that the adsorption of MB on the obtained activated carbon samples is described by the pseudo-second order model. The kinetic constant of the pseudo-second order kinetic model describes the rate of the chemical reaction; the higher the kinetic constant, the faster the reaction (Tien et al. 2017). For samples AC_K and AC_P the kinetic constant of second order was 6.94×10^{-4} [g/mg × min], while for sample AC_{Na} it was 1.81×10^{-3} [g/mg × min], which indicates that the process of MB adsorption on sample AC_{Na} was much slower than on the other two samples.

Thermodynamic study

Figure 10 presents the effect of temperature on the sorption capacities of the studied activated carbon samples. With increasing temperature the effectiveness of MB removal by adsorption on the studied samples increases as well. This relation is particularly well pronounced for sample AC_{Na}. At 60 oC the sorption capacities of samples AC_{Na} and AC_P are very similar, of 75 and 78 mg/g, respectively, although their textural parameters are significantly different, (Table 4). The sorption capacity of sample AC_{Na} at 60 °C was by 83% greater than at 45 °C. The effect of increasing temperature on the sorption capacities of samples AC_K and AC_P was insignificant, which is economically beneficial as it means that the process is effective at room temperature and does not need additional energy expenditure.

The data presented in Table 9 imply that for all activated carbon samples studied the process of adsorption is spontaneous, which is supported by the negative value of free enthalpy (ΔG^o) that decreases with increasing temperature. The effectiveness of capturing of MB molecules from aqueous solution increases with increasing temperature, so the process is endothermic. It is confirmed by the positive values of the adsorption enthalpy (ΔH^o, Table 9). With increasing temperature of the process of adsorption the rate of diffusion of MB molecules increases as does the sorption capacity of the obtained activated carbon samples. Entropy ΔS is a measure of a system disorder and also has an impact on the adsorption process in which MB molecules are attracted to and bonded to the adsorbent surface. The degree of disordering of the activated carbon samples obtained by chemical activation of fennel seeds increases in the order $AC_P < AC_{Na} < AC_K$.

Mechanisms of adsorption

This section provides an explanation of the adsorption mechanism of MB. The pH of the solution plays a crucial

Fig. 8 The effect of pH on the adsorption of methylene blue (biocarbon mass: 25 mg, initial dye solution concentration: 40 mg/L for AC_{Na} and AC_P, 200 mg/L for AC_K, methylene blue solution volume: 50 mL, temperature: 23 ± 1 °C)
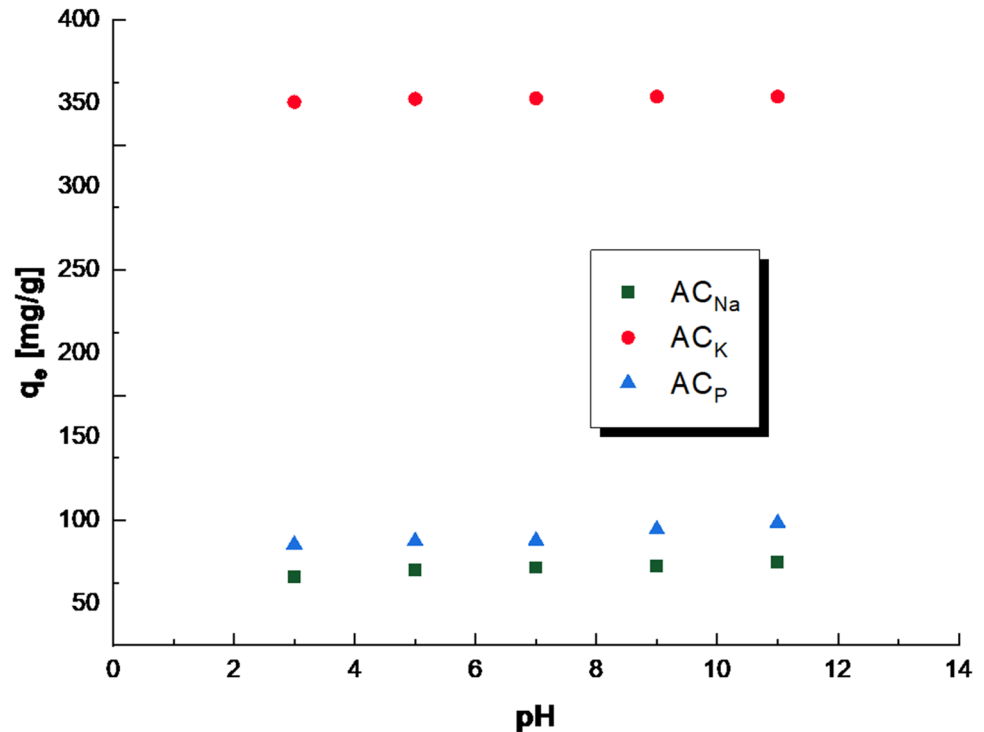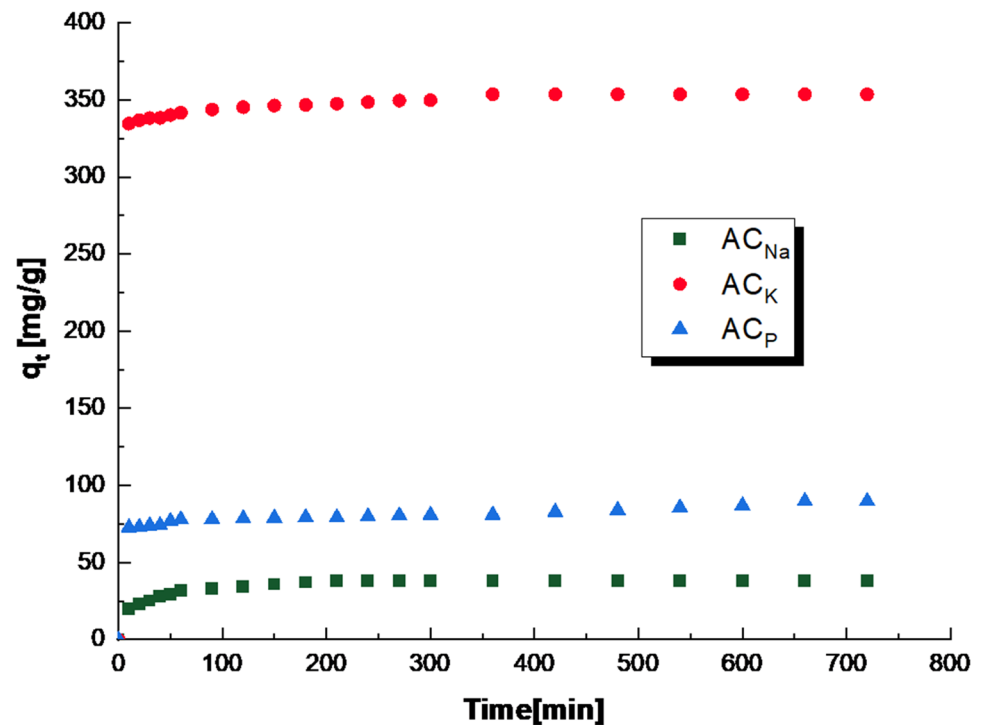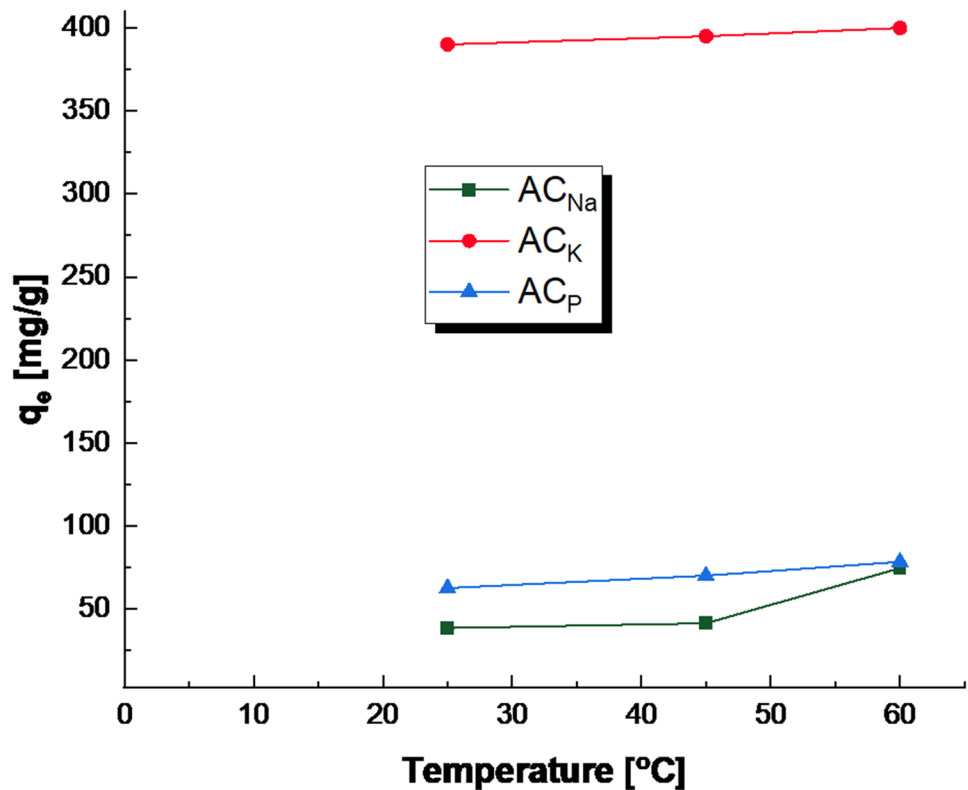

Fig. 9 The effect of contact time of biocarbon with methylene blue (biocarbon mass: 25 mg, initial dye solution concentration: 40 mg/L for AC_{Na}, 40 for AC_P and 200 for AC_K volume of methylene blue solution: 50 mL, temperature: 23 ± 1 °C)

role in the electrostatic interaction between the adsorbent and MB. The acidity dissociation constant (pKa) of MB is 3.14 (PubChem). The net charge on the adsorbent surface, determined by the isoelectric point, influences the nature of the interaction. At pH values higher than the isoelectric point, the adsorbent surface carries a net negative charge, facilitating electrostatic attraction and absorption of MB. Consequently, the optimal pH for MB absorption can sometimes be as low as 10–11 (Iwuozor et al. 2021). π–π interactions occur between the adsorbent's benzene ring

Table 8 Kinetic models parameters

Sample	q_e [mg/g]	Pseudo-first-order kinetics			Pseudo-second-order kinetics		
		k_1 [1/min]	R^2	$q_{e/cal}$ [mg/g]	R^2	k_2 [g/mg × min]	$q_{e/cal}$ [mg/g]
AC_{Na}	38	1.54×10^{-2}	0.978	20	0.999	1.81×10^{-3}	39
AC_K	354	5.29×10^{-3}	0.981	17	0.999	6.94×10^{-4}	357
AC_P	90	2.07×10^{-3}	0.845	16	0.997	6.94×10^{-4}	91

Fig. 10 Temperature influence on the adsorption of methylene blue (biocarbon mass: 25 mg, initial dye solution concentration: 40 mg/L for AC_{Na} and AC_P, 200 mg/L fpr AC_K, methylene blue solution volume: 50 mL, temperature: 23 ± 1 °C)

Table 9 Thermodynamical parameters of MB adsorption from aqueous solution on the carbon adsorbents studied

Sample	Temperature [°C]	ΔG^o [kJ/mol]	ΔH^o [kJ/mol]	ΔS^o [J/mol × K]
AC_{Na}	25	− 1.52	59.19	200.48
	45	− 2.00		
	60	− 9.32		
AC_K	25	− 15.88	88.90	344.57
	45	− 15.09		
	60	− 29.78		
AC_P	25	− 4.81	48.87	178.78
	45	− 6.93		
	60	− 11.50		

and MB (Fig. 11), facilitated by MB's three benzene rings (with substituted carbons) (Jawad et al. 2021). Electronegative heteroatoms in MB, such as nitrogen and sulfur, can form hydrogen bonds with functional groups on the adsorbent surface. π-π interactions between the benzene rings of the adsorbent and methylene blue, as well as hydrogen bonding with electronegative heteroatoms in MB, are important for adsorption. The hydrophobic effect is less significant due to MB's high solubility (Iwuozor et al. 2021).

Conclusions

Characterization of the carbon adsorbents obtained from fennel seeds by chemical activation with potassium carbonate, sodium carbonate or a 50% solution of phosphoric(V) acid was performed. The choice of activating reagent

Fig. 11 The adsorption mechanisms of methylene blue by adsorbents
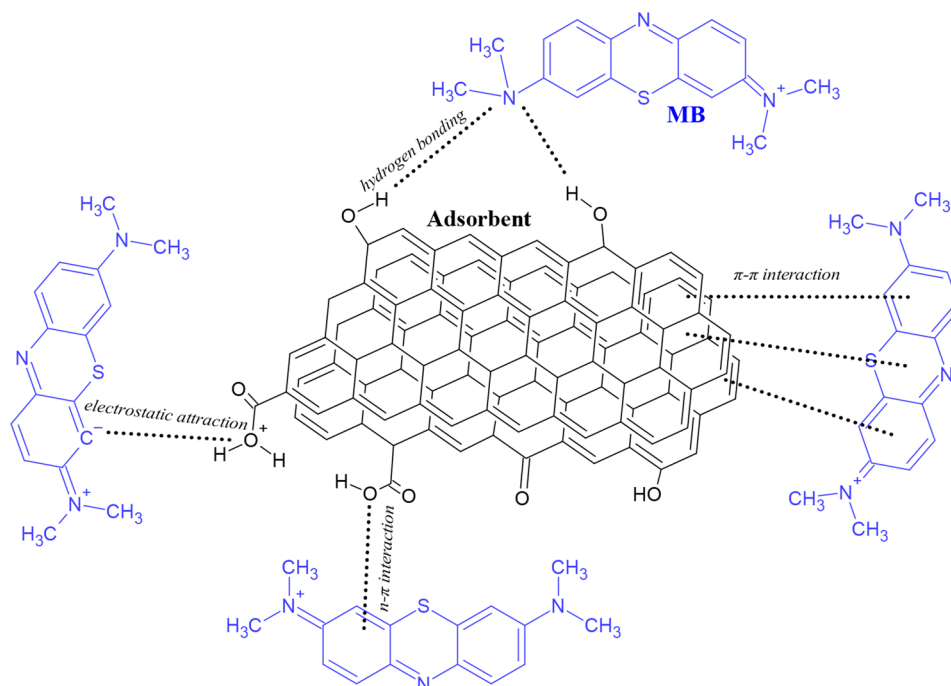
influenced the textural parameters of the activated carbon samples. Samples AC_P and AC_K exhibited higher sorption capacities for iodine (1196 mg/g and 1215 mg/g, respectively) compared to AC_{Na} (317 mg/g). The adsorption of MB from water followed the Langmuir model, forming a monolayer on the adsorbent surface. The sorption capacities for MB were 474 mg/g (AC_K), 122 mg/g (AC_P), and 77 mg/g (AC_{Na}). The adsorbent-adsorbate interactions followed the pseudo-second order model, irrespective of the pH of the MB solution, while increasing temperatures enhanced sorption capacities and indicated an endothermic and spontaneous adsorption process. Analysis of the data characterizing the obtained activated carbon adsorbents shows that the sample obtained by the precursor activation with potassium carbonate can be particularly effective and economic adsorbent of toxic organic dyes from aqueous solutions.

Declarations

Conflict of interest On behalf of all authors, the corresponding author states that there is no conflict of interest.

References

Al-Ghouti MA, Da'ana DA (2020) Guidelines for the use and interpretation of adsorption isotherm models: a review. J Hazard Mater 393:122383. https://doi.org/10.1016/j.jhazmat.2020.122383

Alves LA, de Castro AH, de Mendonça FG, de Mesquita JP (2016) Characterization of acid functional groups of carbon dots by nonlinear regression data fitting of potentiometric titration curves. Appl Surf Sci 370:486–495. https://doi.org/10.1016/j.apsusc.2016.02.128

BalAltuntaş D, Nevruzoğlu V, Dokumacı M, Cam Ş (2020) Synthesis and characterization of activated carbon produced from waste human hair mass using chemical activation. Carbon Lett 30(3):307–313. https://doi.org/10.1007/s42823-019-00099-9

Bazan A, Nowicki P, Pietrzak R (2017) The influence of activation procedure on the physicochemical and sorption properties of activated carbons prepared from pistachio nutshells for removal of NO_2/H_2S gases and dyes. J Clean Prod 152:211–222. https://doi.org/10.1016/j.jclepro.2017.03.114

Bazan-Wozniak A, Nowicki P, Pietrzak R (2018) Production of new activated bio-carbons by chemical activation of residue left after supercritical extraction of hops. Environ Res 161:456–463. https://doi.org/10.1016/j.envres.2017.11.041

Bazan-Wozniak A, Wolski R, Paluch D, Nowicki P, Pietrzak R (2022) Removal of organic dyes from aqueous solutions by activated carbons prepared from residue of supercritical extraction of marigold. Materials 15(10):3655. https://doi.org/10.3390/ma15103655

Bhattacharya R (2023) A review on production and application of activated carbon from discarded plastics in the context of 'waste treats waste'. J Environ Manage325:116613. https://doi.org/10.1016/j.jenvman.2022.116613

Cabrita I, Ruiz B, Mestre AS, Fonseca IM, Carvalho AP, Ania CO (2010) Removal of an analgesic using activated carbons prepared from urban and industrial residues. Chem Eng J 163(3):249–255. https://doi.org/10.1016/j.cej.2010.07.058

Canales-Flores RA, Prieto-García F (2020) Taguchi optimization for production of activated carbon from phosphoric acid impregnated agricultural waste by microwave heating for the removal of methylene blue. Diam Relat Mater109:108027. https://doi.org/10.1016/j.diamond.2020.108027

Danish M, Pin Z, Ziyang L, Ahmad T, Majeed S, Yahya ANA, Khalil HA (2022) Preparation and characterization of banana trunk activated carbon using H_3PO_4 activation: a rotatable central composite design approach. Mater Chem Phys 282:25989. https://doi.org/10.1016/j.matchemphys.2022.125989

Doczekalska B, Bartkowiak M, Łopatka H, Zborowska M (2022a) Activated Carbon Prepared from Corn Biomass by Chemical Activation with Potassium Hydroxide. BioResour 17(1). https://doi.org/10.15376/biores.17.1.1794-1804

Ezzati R (2020) Derivation of pseudo-first-order, pseudo-second-order and modified pseudo-first-order rate equations from Langmuir and Freundlich isotherms for adsorption. Chem Eng J 392:123705. https://doi.org/10.1016/j.cej.2019.123705

Foo KY, Hameed BH (2012) Preparation, characterization and evaluation of adsorptive properties of orange peel based activated carbon via microwave induced K_2CO_3 activation. Bioresour Technol 104:679–686. https://doi.org/10.1016/j.biortech.2011.10.005

Gao Y, Yue Q, Gao B, Li A (2020) Insight into activated carbon from different kinds of chemical activating agents: A review. Sci Total Environ 746:141094. https://doi.org/10.1016/j.scitotenv.2020.141094

Gupta SA, Vishesh Y, Sarvshrestha N, Bhardwaj AS, Kumar PA, Topare NS, Khan A (2022) Adsorption isotherm studies of Methylene blue using activated carbon of waste fruit peel as an adsorbent. Mater Today: Proc 57:1500–1508. https://doi.org/10.1016/j.matpr.2021.12.044

Heidarinejad Z, Dehghani MH, Heidari M, Javedan G, Ali I, Sillanpää M (2020) Methods for preparation and activation of activated carbon: a review. Environ Chem Lett 18(2):393–415. https://doi.org/10.1007/s10311-019-00955-0

Hussaro K (2014) Preparation of activated carbon from palm oil shell by chemical activation with Na_2CO_3 and $ZnCl_2$ as impregnated agents for H_2S adsorption. Am J Environ Sci 10(4):336–346. https://doi.org/10.3844/ajessp.2014.336.346

Ikram M, Naeem M, Zahoor M, Rahim A, Hanafiah MM, Oyekanmi AA, Sadiq A (2022) Biodegradation of Azo Dye Methyl Red by Pseudomonas aeruginosa: Optimization of Process Conditions. Int J Environ Res Public Health 19(16):9962. https://doi.org/10.3390/ijerph19169962

Ishak Z, Kumar D (2022) Adsorption of Methylene Blue and Reactive Black 5 by Activated Carbon Derived from Tamarind Seeds. Trop Aqua Soil Pollut 2(1):1–12. https://doi.org/10.53623/tasp.v2i1.26

Iwuozor KO, Ighalo JO, Ogunfowora LA, Adeniyi AG, Igwegbe CA (2021) An empirical literature analysis of adsorbent performance for methylene blue uptake from aqueous media. J Environ Chem Eng 9(4):105658. https://doi.org/10.1016/j.jece.2021.105658

Jawad AH, Abdulhameed AS, Wilson LD, Syed-Hassan SSA, ALOthman ZA, Khan MR (2021) High surface area and mesoporous activated carbon from KOH-activated dragon fruit peels for methylene blue dye adsorption: Optimization and mechanism study. Chin J Chem Eng32:281–290.https://doi.org/10.1016/j.cjche.2020.09.070

Khan JH, Marpaung F, Young C, Lin J, Islam MT, Alsheri SM, Kim J (2019) Jute-derived microporous/mesoporous carbon with ultra-high surface area using a chemical activation process. Microporous Mesoporous Mater 274:251–256. https://doi.org/10.1016/j.micromeso.2018.07.050

Khan RU, Fatima A, Naz S, Ragni M, Tarricone S, Tufarelli V (2022a) Perspective, Opportunities and Challenges in Using Fennel (*Foeniculum vulgare*) in Poultry Health and Production as an Eco-Friendly Alternative to Antibiotics: A Review. Antibiotics 11(2):278. https://doi.org/10.3390/antibiotics11020278

Khan TA, Nouman M, Dua D, Khan SA, Alharthi SS (2022b) Adsorptive scavenging of cationic dyes from aquatic phase by H_3PO_4 activated Indian jujube (*Ziziphus mauritiana*) seeds based activated carbon: Isotherm, kinetics, and thermodynamic study. J Saudi Chem Soc26(2):101417. https://doi.org/10.1016/j.jscs.2021.101417

Mahardiani L, Saputro S, Baskoro F, Zinki NM, Taufiq M (2019) Facile synthesis of carboxylated activated carbon using green approach for water treatment. IOP Conf Ser Mater Sci Eng 578(1):012003. https://doi.org/10.1088/1757-899X/578/1/012003

Medhat A, El-Maghrabi HH, Abdelghany A, Menem NMA, Raynaud P, Moustafa YM, Nada AA (2021) Efficiently activated carbons from corn cob for methylene blue adsorption. Appl Surf Sci Adv3:100037. https://doi.org/10.1016/j.apsadv.2020.100037

Misran E, Bani O, Situmeang EM, Purba AS (2022) Banana stem based activated carbon as a low-cost adsorbent for methylene blue removal: Isotherm, kinetics, and reusability. Alex Eng J 61(3):1946–1955. https://doi.org/10.1016/j.aej.2021.07.022

Naji SZ, Tye CT (2022b) A review of the synthesis of activated carbon for biodiesel production: Precursor, preparation, and modification. Energy Convers Manag 10(13):100152. https://doi.org/10.1016/j.ecmx.2021.100152

Nowicki P, Bazan A, Kazmierczak-Razna J, Pietrzak R (2015) Sorption properties of carbonaceous adsorbents obtained by pyrolysis and activation of pistachio nut shells. Adsorp Sci Technol 33(6–8):581–586. https://doi.org/10.1260/0263-6174.33.6-8.581

Pathania D, Sharma S, Singh P (2017) Removal of methylene blue by adsorption onto activated carbon developed from Ficus carica bast. Arab J Chem 10:1445–1451. https://doi.org/10.1016/j.arabjc.2013.04.021

PubChem, Methylene Blue, 2021 [cited 18th May 2022]. Available from: https://pubchem.ncbi.nlm.nih.gov/compound/Methylene-blue

Queiroz LS, de Souza LK, Thomaz KTC, Lima ETL, da Rocha Filho GN, do Nascimento LAS. da Costa CE (2020) Activated carbon obtained from amazonian biomass tailings (acai seed): Modification, characterization, and use for removal of metal ions from water. J Environ Manage 270:110868. https://doi.org/10.1016/j.jenvman.2020.110868

Ramutshatsha-Makhwedzha D, Mavhungu A, Moropeng ML, Mbaya R (2022) Activated carbon derived from waste orange and lemon peels for the adsorption of methyl orange and methylene blue dyes from wastewater. Heliyon 8(8):e09930. https://doi.org/10.1016/j.heliyon.2022.e09930

Schurr L, Masotti V, Geslin B, Gachet S, Mahé P, Jeannerod L, Affre L (2022) To what extent is fennel crop dependent on insect pollination?. AgricuEcosyst Environ338:108047. https://doi.org/10.1016/j.agee.2022.108047

Sekirifa ML, Hadj-Mahammed M, Pallier S, Baameur L, Richard D, Al-Dujaili AH (2013) Preparation and characterization of an activated carbon from a date stones variety by physical activation with carbon dioxide. J Anal Appl Pyrolysis 99:155–160. https://doi.org/10.1016/j.jaap.2012.10.007

Sevilla M, Díez N, Fuertes AB (2021) More sustainable chemical activation strategies for the production of porous carbons. ChemSusChem14(1):94–117. https://doi.org/10.1002/cssc.202001838

Springer

Shi Y, Song G, Li A, Wang J, Wang H, Sun Y, Ding G (2022) Graphene oxide-chitosan composite aerogel for adsorption of methyl orange and methylene blue: Effect of pH in single and binary systems. Colloids Surf A PhysicochemEng Asp 641:128595. https://doi.org/10.1016/j.colsurfa.2022.128595

Sych NV, Trofymenko SI, Poddubnaya OI, Tsyba MM, Sapsay VI, Klymchuk DO, Puziy AM (2012) Porous structure and surface chemistry of phosphoric acid activated carbon from corncob. Appl Surf Sci 261:75–82. https://doi.org/10.1016/j.apsusc.2012.07.084

Thommes M, Kaneko K, Neimark AV, Olivier JP, Rodriguez-Reinoso F, Rouquerol J, Sing KS (2015) Physisorption of gases, with special reference to the evaluation of surface area and pore size distribution (IUPAC Technical Report). Pure Appl Chem 87(9–10):1051–1069. https://doi.org/10.1515/pac-2014-1117

Tien C, Ramarao BV (2017) On the significance and utility of the Lagergren model and the pseudo second-order model of batch adsorption. Sep Sci Technol 52(6):975–986. https://doi.org/10.1080/01496395.2016.1274327

Tounsadi H, Khalidi A, Machrouhi A, Farnane M, Elmoubarki R, Elhalil A, Barka N (2016). Highly efficient activated carbon from Glebionis coronaria L. biomass: Optimization of preparation conditions and heavy metals removal using experimental design approach. J Environ Chem Eng4(4):4549–4564.https://doi.org/10.1016/j.jece.2016.10.020

Tran HN, Chao HP, You SJ (2018) Activated carbons from golden shower upon different chemical activation methods: synthesis and characterizations. Adsorp Sci Technol 36(1–2):95–113. https://doi.org/10.1177/0263617416684837

Vassilev SV, Baxter D, Andersen LK, Vassileva CG (2013) An overview of the composition and application of biomass ash. Part 1. Phase–mineral and chemical composition and classification. Fuel 105:40–76. https://doi.org/10.1016/j.fuel.2012.09.041

Vilén A, Laurell P, Vahala R (2022) Comparative life cycle assessment of activated carbon production from various raw materials. J Environ Manage 324:116356. https://doi.org/10.1016/j.jenvman.2022.116356

Villabona-Ortíz Á, Figueroa-Lopez KJ, Ortega-Toro R (2022) Kinetics and adsorption equilibrium in the removal of azo-anionic dyes by modified cellulose. Sustainability 14:3640. https://doi.org/10.3390/su14063640

Publisher's Note Springer Nature remains neutral with regard to jurisdictional claims in published maps and institutional affiliations.